Available online at www.sciencedirect.com
SCIENCE DIRECT
Geomorphology 75 (2006) 346–367
GEOMORPHOLOGY
www.elsevier.com/locate/geomorph

Late Pleistocene outburst flooding from pluvial Lake Alvord into the Owyhee River, Oregon

Deron T. Carter [a,*], Lisa L. Ely [a], Jim E. O'Connor [b], Cassandra R. Fenton [c]

[a] *Department of Geological Sciences, Central Washington University, Ellensburg, Washington, USA*
[b] *U.S. Geological Survey, Portland, Oregon, USA*
[c] *U.S. Geological Survey, Tucson, Arizona, USA*

Accepted 27 July 2005
Available online 14 February 2006

Abstract

At least one large, late Pleistocene flood traveled into the Owyhee River as a result of a rise and subsequent outburst from pluvial Lake Alvord in southeastern Oregon. Lake Alvord breached Big Sand Gap in its eastern rim after reaching an elevation of 1292 m, releasing 11.3 km^3 of water into the adjacent Coyote Basin as it eroded the Big Sand Gap outlet channel to an elevation of about 1280 m. The outflow filled and then spilled out of Coyote Basin through two outlets at 1278 m and into Crooked Creek drainage, ultimately flowing into the Owyhee and Snake Rivers. Along Crooked Creek, the resulting flood eroded canyons, stripped bedrock surfaces, and deposited numerous boulder bars containing imbricated clasts up to 4.1 m in diameter, some of which are located over 30 m above the present-day channel.

Critical depth calculations at Big Sand Gap show that maximum outflow from a 1292- to 1280-m drop in Lake Alvord was ~10,000 $m^3\ s^{-1}$. Flooding became confined to a single channel approximately 40 km downstream of Big Sand Gap, where step-backwater calculations show that a much larger peak discharge of 40,000 $m^3\ s^{-1}$ is required to match the highest geologic evidence of the flood in this channel. This inconsistency can be explained by (1) a single 10,000 $m^3\ s^{-1}$ flood that caused at least 13 m of vertical incision in the channel (hence enlarging the channel cross-section); (2) multiple floods of 10,000 $m^3\ s^{-1}$ or less, each producing some incision of the channel; or (3) an earlier flood of 40,000 $m^3\ s^{-1}$ creating the highest flood deposits and crossed drainage divides observed along Crooked Creek drainage, followed by a later 10,000 $m^3\ s^{-1}$ flood associated with the most recent shorelines in Alvord and Coyote Basins.

Well-developed shorelines of Lake Alvord at 1280 m and in Coyote Basin at 1278 m suggest that after the initial flood, postflood overflow persisted for an extended period, connecting Alvord and Coyote Basins with the Owyhee River of the Columbia River drainage. Surficial weathering characteristics and planktonic freshwater diatoms in Lake Alvord sediment stratigraphically below Mt. St. Helens set Sg tephra, suggest deep open-basin conditions at ~13–14 ka (^{14}C yr) and that the flood and prominent shorelines date to about this time. But geomorphic and sedimentological evidence also show that Alvord and Coyote Basins held older, higher-elevation lakes that may have released earlier floods down Crooked Creek.

Keywords: Lake Alvord; Pluvial; Outburst flood; Paleohydrology

1. Introduction

Large Pleistocene floods have substantially influenced many portions of the landscape of the western

* Corresponding author. Current address: Department of Earth and Physical Sciences, Western Oregon University, Monmouth, Oregon, USA.
E-mail address: carterd@wou.edu (D.T. Carter).

0169-555X/$ - see front matter © 2006 Elsevier B.V. All rights reserved.
doi:10.1016/j.geomorph.2005.07.023

United States. The widespread effects of some the largest floods are well documented. The Missoula Floods, resulting from the repeated draining of ice-dammed glacial Lake Missoula, altered the course of major drainages, including the Columbia River, and created the extensive Channeled Scabland of eastern Washington State (e.g. Bretz, 1969; Baker, 1973). Lake Bonneville, the largest pluvial lake in the western U.S., overtopped Redrock Pass and sent a cataclysmic flood down the Snake River about 15,000 ^{14}C yrs ago, locally altering the river course and eroding spectacular cataracts and scabland topography (Malde, 1968; O'Connor, 1993). Other floods of smaller magnitude, but also from various types of failures of natural dams, have significantly altered regional landscapes within watersheds and fluvial corridors, such as lava-dam outburst floods on the Colorado River (Fenton et al., 2003), and the Big Lost River Flood in Idaho (Rathburn, 1993; Knudsen et al., 2002). In most cases, floods from such lake outbursts are much larger than meteorological floods; consequently they have the capacity to radically modify landscapes, including cutting canyons, creating new drainage courses, and establishing or severing hydrologic connections that can affect ecological conditions. Large-magnitude nonmeteorological floods are especially important in regions such as western North America, where glaciation, tectonism and volcanism have produced numerous lakes and closed basins susceptible to filling and spilling. The late Pleistocene produced particularly frequent floods of this scale because of the formation of large ice- or debris-dammed lakes (O'Connor et al., 2002).

Another example of such a flood resulted from the spillover of Pluvial Lake Alvord into Crooked Creek, a tributary of the Owyhee River in southeastern Oregon. Here, we report an analysis of the flood, including the age and magnitude of overflow, analysis of downstream effects, and the relation of flooding to the history of Pluvial Lake Alvord.

2. Study area

The once-connected hydrologic system of pluvial Lakes Alvord and Coyote and Crooked Creek drainage to the east are within the northernmost Great Basin in southeastern Oregon (Fig. 1). Pluvial Lake Alvord was over 130-km long and as deep as 86 m during its highest evident Pleistocene stand of 1310 m (meters above sea level), covering much of the present-day closed basins of Alvord and Pueblo valleys and numerous other subbasins (Fig. 1; Russell, 1884, 1903; Hubbs and Miller, 1948, Hemphill-Haley, 1987; Hemphill-Haley et al., 1999; Lindberg, 1999, Marith Reheis, U.S. Geological Survey, personal communication, 2003; Personius et al., 2004). The lake basin was bound on the west by the Steens Mountain range, with a crest at 2966 m, and by the lower Pueblo Mountains on the southwest.

Coyote Basin, immediately east of Alvord Basin, also contained lakes during the Pleistocene. At its maximum level of 1292 m, pluvial Lake Coyote was 25 km long and 42 m deep. The relatively small drainage area for Coyote Basin makes it unlikely to have substantial water volumes except when supplied by spillover from Lake Alvord via Big Sand Gap (Hemphill-Haley, 1987). Much of present-day direct runoff into Coyote Basin is from the Trout Creek Mountains to the south (Fig. 1).

East of Coyote Basin, Crooked Creek is now an intermittent stream that largely originates from Crooked Creek Spring and flows northeasterly through semiarid sagebrush steppe into the Owyhee River (Fig. 1). For several reaches, the creek flows through deep canyons incised in Tertiary and Quaternary basalts and Tertiary semiconsolidated tuffaceous, fluvial, and lacustrine sediment (Walker and Repenning, 1966).

Overflow of pluvial Lake Alvord into Crooked Creek by way of Big Sand Gap and Coyote Basin was suggested by Smith and Young (1926), Hemphill-Haley (1987), Lindberg and Hemphill-Haley (1988) and Behnke (1992), while evidence for a large downstream flood associated with overflow was described by Hemphill-Haley et al. (1999), Lindberg (1999), and Marith Reheis (U.S. Geological Survey, personal communication, 2003), but no detailed assessment of the extent, hydrology, and chronology of the flood had been previously undertaken.

3. Field methods

On the basis of reconnaissance observations of flood evidence along Crooked Creek by Hemphill-Haley et al. (1999) and Marith Reheis (U.S. Geological Survey, written communications, 1999), we mapped pluvial lake and flood features from 1:72,000-scale aerial photographs. Based on this photo analysis, we conducted field mapping for select areas on 1:24,000-scale U.S. Geological Survey topographic maps. Our primary emphasis was to determine locations and altitudes of geologic evidence of flood limits and paleolake stages. Positions and elevations were determined by (1) handheld global positioning system (GPS) acquisition of location, with elevation determined from the corresponding elevations shown on 1:24,000 scale

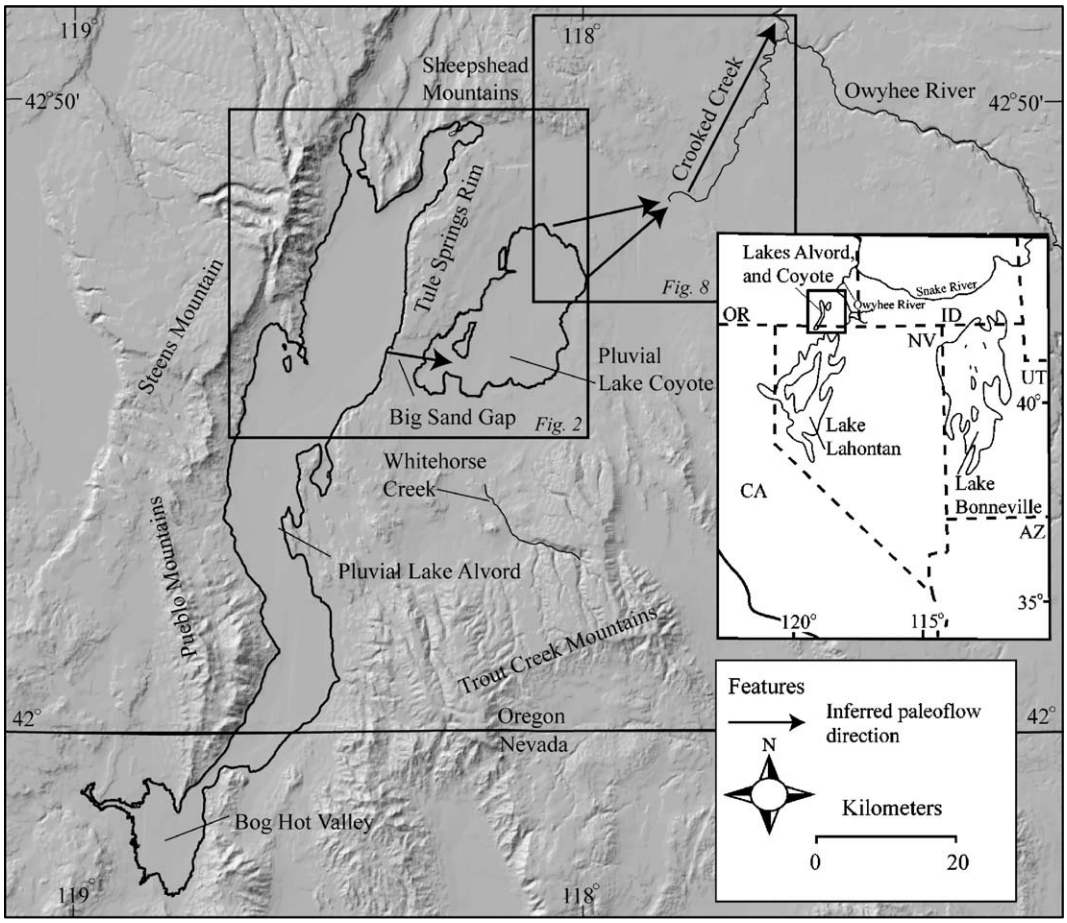

Fig. 1. Location map of Lakes Alvord and Coyote, showing Pleistocene high stands at 1310 m and 1292 m, respectively, and direction of flood overflow into the Owyhee River (adapted from Oviatt, 1997; Reheis, 1999). Boxes indicate locations for Figs. 2 and 8.

U.S. Geological Survey topographic maps with 10- or 20-ft. contour intervals; (2) hand level, altimeter, and tape-and-inclinometer surveys of features near spot elevations and benchmarks shown on USGS topographic maps; and (3) precise point kinematic (PPK) GPS surveys at valley constrictions suitable for step-backwater hydraulic modeling.

4. Pluvial Lakes Alvord and Coyote

The two major, closely related components of this study were assessment of the pluvial lake history and outlet conditions for Lakes Alvord and Coyote, and determination of the magnitude and effects of overflow into Crooked Creek drainage. This lake-level analysis builds on recent studies by Hemphill-Haley (1987) and Lindberg (1999, Table 1). We examined elevations and weathering characteristics of preserved lakeshore features such as wave-cut shoreline notches, beach barrier bars, spits, tombolos, and back-barrier lagoons in the northern Alvord Basin and Coyote Basin to determine elevations and relative age of prominent stillstands in both basins, and the relation to Big Sand Gap, a short, narrow channel which forms the lowest connection between the two basins (Fig. 2). Shoreline features were correlated across the basins based on similar altitudes, degree of landform preservation, surficial characteristics such as weathering, carbonate and rock varnish development, and soil characteristics. Emphasis was placed on constructional shoreline features for relative dating, as these generally contain deposits and landforms (Adams and Wesnousky, 1999).

4.1. Pluvial Lake Alvord shorelines

Five prominent paleoshorelines are evident in the northern Alvord Basin at altitudes of 1310, 1305, 1292, 1287, and 1280 m. Paleoshorelines at 1292 m and 1280 m are strongly developed, suggesting that pluvial Lake

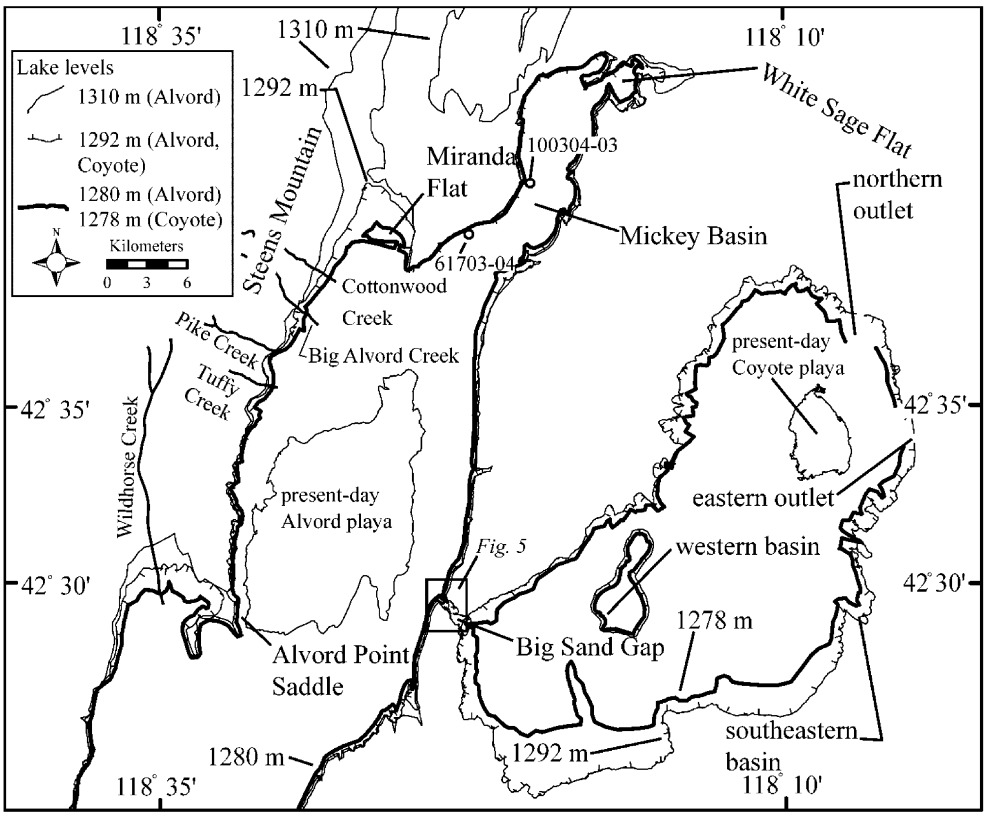

Fig. 2. Shoreline map of Lakes Alvord and Coyote. Sites 61703-04 and 100304-03 were sampled for tephrochronology. Box indicates location of Fig. 5.

Alvord persisted at these elevations for extended periods of time, probably with outlets at these elevations (Table 1; Fig. 2).

The 1310-m shoreline represents the highest obvious stand of Lake Alvord. Evidence for this shoreline includes a degraded wave-cut bench in basalt near Tuffy Creek and along Alvord Point on the western edge of Alvord Basin (Hemphill-Haley, 1987) (Fig. 2), and shoreline features in Bog Hot Valley at the southern end of the basin (Personius et al., 2004) (Fig. 1). A deposit of highly weathered, rounded and subrounded gravels with stage II+ pedogenic carbonate development at 1305 m near Alvord Point Saddle may be associated with this lake stand as well (Fig. 2). Lindberg (1999) also noted a shoreline at 1302 m at Little Sand Gap (Fig. 2).

A very prominent shoreline in Alvord Basin occurs at about 1292 m. Extensive and laterally continuous barrier beaches were observed in the present study at 1292 m in the Mickey Basin and Miranda Flat. Personius et al. (2004) also described lacustrine deposits at 1292 m in Bog Hot Valley, and Lindberg (1999) identified a shoreline at 1294 m at Little Sand Gap (Table 1; Figs. 1 and 2). The shorelines at 1292 m observed in this study are well-preserved landforms, with surficial clasts that have discontinuous varnish and pedogenic carbonate accumulations (stage I). A shallow excavation (>75 cm) in a spit in Mickey Basin at 1292 m shows a weak Av horizon and little development of an argillic horizon. A trench in Bog Hot Valley, at the southern end of Alvord Basin, showed well-stratified lacustrine silt, sand, and gravel at 1292 m, with a maximum stage I–II Bk horizon development (Personius et al., 2004). Lindberg's (1999) study did not focus on the relative age of the 1294-m shoreline at Little Sand Gap, so its relation to the others at 1292 m is unclear.

Shoreline features at 1287 m were found at only one location in this study, a well-preserved spit approximately 2.4 km long at Miranda Flat (Table 1; Fig. 2). Lindberg (1999) noted a paleoshoreline at 1287 m in the Mickey Basin, but we could not find this level in our reconnaissance of the area (Table 1). The sedimentology and weathering characteristics of the shorelines at 1287 m and 1292 m are similar, precluding us from determining whether the 1287-m paleoshoreline pre- or postdates the 1292-m shoreline. The limited expression

Table 1
Paleoshoreline elevations for the northern Alvord and Coyote Basins

Elevation (m)	Location
Alvord Basin	
1310-m paleoshoreline	
1310[a]	Tuffy Creek
1305-m paleoshoreline	
1305[a,b]	Alvord Point Saddle
1292-m paleoshoreline suite	
1292[b]	Mickey Basin
1292[b]	Miranda Flat
1291[c]	Mickey Basin
1290[c]	White Sage Flat
1287-m paleoshoreline suite	
1287[b]	Miranda Flat
1287[c]	Mickey Basin
1280-m paleoshoreline suite	
1283[c]	White Sage Flat
1283[b,c]	Miranda Flat
1280[b]	White Sage Flat
1280[a,b]	Big Sand Gap
1280[a]	Wildhorse Creek
1280[a]	Pike Creek
1280[a]	Big Alvord Creek
1280[a]	Cottonwood Creek
1279[c]	Mickey Basin
1276[b]	Mickey Basin
Coyote Basin	
1292[b]	Western basin
1278[b]	Near outlets
1289[b]	Southeastern basin

[a] From Hemphill–Haley, 1987.
[b] From this study.
[c] From Lindberg, 1999.

of the 1287-m shoreline may indicate it formed during a brief stillstand during the transgression of Lake Alvord its 1292-m stage, and was buried or eroded as the lake continued to rise. Alternatively, the 1287-m shoreline could be younger than the 1292-m shoreline, and simply not well preserved in most locations.

The most prominent Lake Alvord paleoshoreline features are at ~1280 m (Table 1; Figs. 2 and 3). Many of these features are continuous throughout subbasins of Alvord Basin, and include (1) spits and laterally continuous barrier bars up to 250 m wide in Mickey Basin, (2) continuous bars and eroded platforms at White Sage Flat, (3) a longitudinal bar 3.4 km long at Miranda Flat, (4) laterally continuous barrier bars as much as 13 m thick and back-barrier lagoon deposits as much as 3 m thick near Big Sand Gap, and (5) large barrier bars at the mouth of Wildhorse, Big Alvord, Cottonwood and Pike Creeks (Hemphill-Haley, 1987; Hemphill-Haley et al., 1989) (Fig. 2; Table 2). These features are correlated based on the prominence and similar weathering characteristics (which are similar to the 1292-m shoreline features), although the present-day elevations of these features range from 1276 m to 1283 m (Table 2). The 7-m range in elevations may result from (1) Quaternary faulting of paleoshorelines (Hemphill-Haley, 1987; Lindberg and Hemphill-Haley, 1988; Hemphill-Haley et al., 1989; Lindberg, 1999; Personius et al., 2004; Singleton and Oldow, 2004), (2) post-pluvial isostatic rebound (Adams, 1997), or to (3) variations in local subbasin geometry and paleowind direction that affected wave fetch and resulting elevation of beach features, similar to that noted by Adams and Wesnousky (1998) in pluvial Lake Lahontan.

4.2. Pluvial Lake Alvord chronology

While we did not conduct detailed soil profile and weathering analyses, the shoreline features at 1292 m, 1287 m, and ~1280 m all show similar weathering characteristics, with little to no varnish or carbonate accumulation and weakly developed soils (Fig. 4). These characteristics are similar to those observed by Adams and Wesnousky (1998, 1999) on Sehoo shorelines related to the last late-Pleistocene highstand of Lake Lahontan, dated at 13.1 ka (^{14}C yr). Because of these similarities, we infer that the 1292-, 1287-, and ~1280-m shorelines related to Lake Alvord more closely resemble a late-Pleistocene age than an older lake cycle, as did Personius et al. (2004) on the basis of soil data on 1292-m lacustrine sediments in Bog Hot Valley.

In addition to reconnaissance observations of soil characteristics, we sampled two tephras from lacustrine deposits in Mickey Basin in the northern part of Lake Alvord Basin. Airfall tephra (sample 61703-04; Fig. 2) sampled from lacustrine silts exposed at 1243 m is geochemically correlative with the Mt. St. Helens set Sg ash (Table 2), indicating that Lake Alvord was >1243 m at the time of the tephra fall. These lacustrine silts suggest a low-energy, deep-water environment at an undetermined depth below the surface of Lake Alvord at the time of tephra deposition. The set Sg tephra was also found by Hemphill-Haley et al. (1989) in a trench near the modern Alvord playa at ~1224 m. The age of the set Sg tephra is not precisely known (Benito and O'Connor, 2003), but has generally been considered to be about ca. 13,000 ^{14}C yrs old on the basis of radiocarbon dating near the volcano (Crandell et al., 1981; Mullineaux, 1986, 1996) and radiocarbon ages of 13,326 ± 185 and 14,060 ± 450 ^{14}C yr B.P. from shells found stratigraphically below Mt. St. Helens set Sg tephra in Missoula Flood rhythmites in Yakima Valley (Baker and Bunker, 1985; Waitt, 1985). Thermoluminenence dating of loess

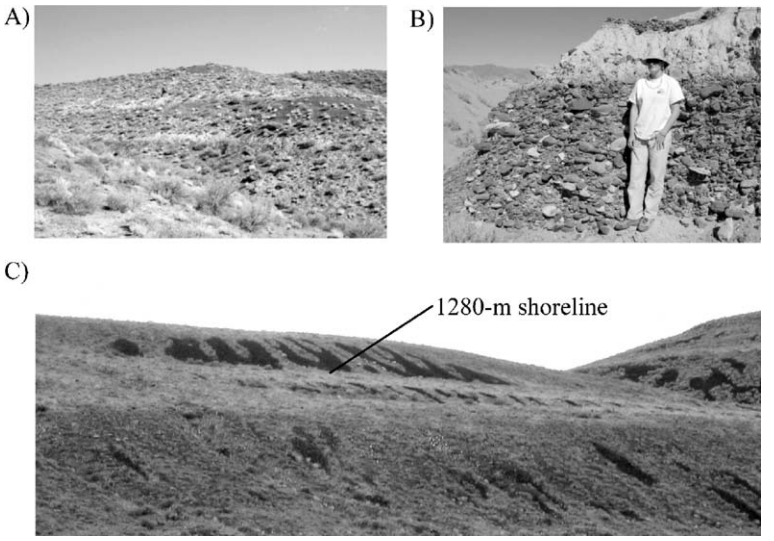

Fig. 3. Lake Alvord paleoshoreline features. (A) Spit, Mickey Basin (approximately 20 m high in photo); (B) back-barrier lagoon (upper unit) inset against barrier (lower unit), Big Sand Gap; (C) bar at 1280 m, White Sage Flat (bar is approximately 300 m long in photo). See Fig. 2 for location of these features.

stratigraphy that brackets the set S tephra in eastern Washington, however, suggests that the tephra may be as much as 18.5 ± 1.5 ka cal. yr B.P. (equivalent to ca. 15,500 ± 1500 ^{14}C yr B.P.) (Berger and Busacca, 1995; Benito and O'Connor, 2003), and tephra deposits located north of the volcano that are geochemically correlative with set S appear to predate 14,000–14,500 ^{14}C yrs B.P. (Beget et al., 1997). In a recent analysis, Clague et al. (2003) estimate the set Sg tephra to have an age ca. 13,350–14,400 ^{14}C yr B.P., on the basis of provisional correlations with secular magnetic variation curves. A second tephra (100304-01) (Fig. 2) sampled from lacustrine silts at ~1276 m and beveled by the 1280-m shoreline could not be geochemically correlated with any known tephras (Nick Foit, Washington State University, personal communication, 2004).

A diatomaceous layer sampled from lacustrine silt 50 cm below Mt. St. Helens set Sg tephra (sample 61703-04) was dominated by *Melosira undulata*. This planktonic species is indicative of clear, fresh to slightly alkaline, nutrient-rich lake conditions (identification and environmental conditions provided by Scott Starratt, U.S. Geological Survey, written communication, 2005). We infer that such freshwater conditions indicate that Lake Alvord was overflowing into Crooked Creek drainage at or slightly before the time of Mt. St. Helens tephra deposition at ~14–13 ^{14}C ka. It is unclear if these open-basin conditions were associated with either the 1292- or 1280-m levels of Lake Alvord, although the first overflow of pluvial Lake Alvord into Crooked Creek drainage must have predated the deposition of Mt. St. Helens set Sg tephra.

Table 2
Glass chemistry of tephra 61703-04 sampled from the Mickey Basin

Sample no.	SiO_2	Al_2O_3	Fe_2O_3	TiO_2	Na_2O	K_2O	MgO	CaO	Cl
61703-04	76.89	13.81	1.24	0.15	3.72	2.19	0.30	1.62	0.08
MSH Sg standard	76.50	13.80	1.29	0.16	4.11	2.14	0.32	1.59	0.09

All values are reported in wt.%. Analysis by Dr. Nick Foit, Washington State University. Similarity coefficient for sample 61703-04 0.97.

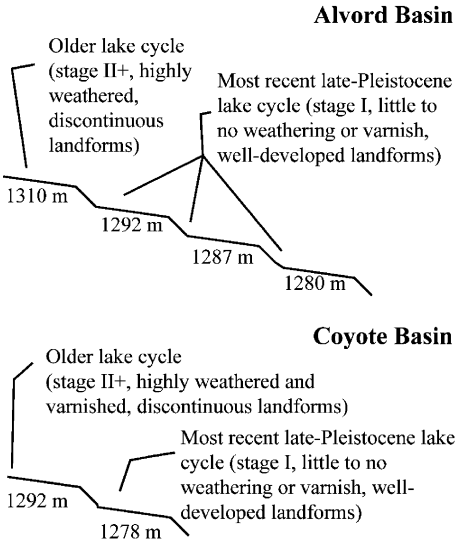

Fig. 4. Idealized chronology for paleoshoreline features in northern Alvord and Coyote Basins. See Table 1 and Fig. 3 for paleoshoreline feature locations.

This timing associated with the 1292-m and 1280-m shorelines is broadly contemporaneous with the Lake Lahonton (in northwestern Nevada) Sehoo highstand at 13.1 ka (^{14}C yr) (Negrini, 2002; Adams and Wesnousky, 1999; Morrison, 1991) and pluvial Lake Chewaucan in south-central Oregon, which achieved its late-Pleistocene highstand 18–16.4 ka (^{14}C yr) (Freidel, 1993). The more subtle and more weathered 1310- to 1305-m Lake Alvord shoreline deposits represent a lake-cycle older than late Pleistocene, and may be correlative with the penultimate Eetza cycle of Lake Lahontan, which Morrison (1991) estimated was between 350 and 130 ka (Fig. 4).

4.3. Big Sand Gap

The particularly strong development of shoreline features at 1292 m and ~1280 m indicate that Lake Alvord maintained constant elevations for substantial durations at those elevations, which in turn indicates lake outlets were controlling lake elevation. Likewise, the prominent but more weathered 1310-m shoreline indicates an older higher outlet. Big Sand Gap was the outlet to pluvial Lake Alvord for at least the late Pleistocene highstands and perhaps earlier highstands as well. Big Sand Gap is a linear pass 90 m deep, 2.3 km long and 300 m wide bisecting the Tule Springs Rim, which separates Alvord and Coyote Basins (Figs. 1 and 2). The present floor of the gap divides Alvord and Coyote Basins at an elevation of 1283 m, but it is partly filled with Holocene eolian sand and alluvial fan deposits (Fig. 5). The 1280-m late-Pleistocene Alvord shoreline almost certainly owes its prominence to a lake level stabilized by overflow through Big Sand Gap in nearly its present configuration (Hemphill-Haley, 1987; Lindberg and Hemphill-Haley, 1988). But what about the higher prominent Alvord shorelines at 1310 m and 1292 m that also suggest stable lake levels? The next highest divide is Little Sand Gap, which closes the Alvord Basin at 1329 m, well above the highest

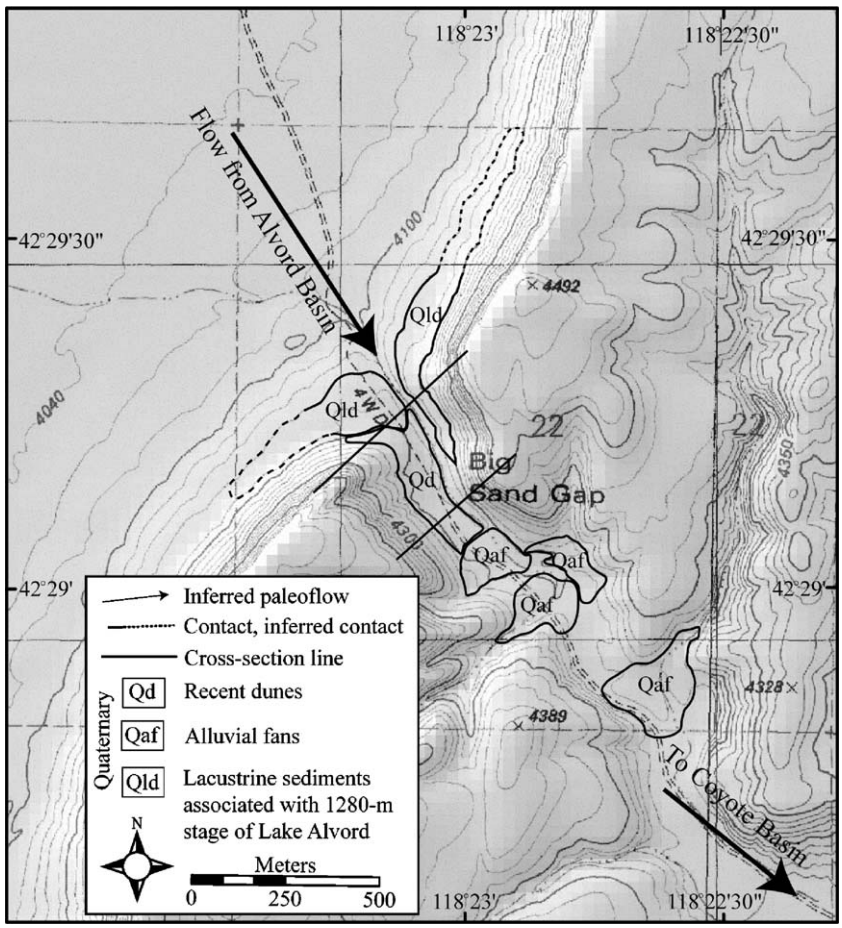

Fig. 5. Geomorphic map of Big Sand Gap and cross-section locations.

known Alvord lake level of 1310 m. Therefore, changing conditions at Big Sand Gap probably controlled outlet conditions for pluvial Lake Alvord throughout the late Pleistocene. These changes may be in part tectonic as suggested by the linear geometry of the gap, but more likely result from a combination of episodic bedrock incision or incision of fluvial or debris-flow sediment deposited in the floor of the gap (between times of high lake level) from tributaries entering from the north and south (Fig. 5).

4.4. Coyote Basin

Coyote Basin is east of Big Sand Gap and would have received spillover at times when pluvial Lake Alvord flowed through Big Sand Gap. Features indicative of two high shorelines are locally preserved in Coyote Basin (Fig. 2; Table 1). The most prominent, continuous suite of shoreline features are barrier beaches, spits, and back-barrier lagoons on the eastern side of Coyote Basin at and just below 1278 m. These features have similar soils (weak Av horizons and little argillic horizon development) and are weathered and varnished to a degree similar to the 1280- and 1292-m shorelines in the Alvord Basin, suggesting a similar late-Pleistocene age (Fig. 4).

A higher shoreline in Coyote Basin at 1292 m is much more subtle and consists of varnished, well-rounded beach cobbles within talus slopes flanking basalt island buttes on the western side of Coyote Basin, and isolated rounded pebbles on the basin margins (Fig. 2). This 1292-m paleoshoreline appears sig-

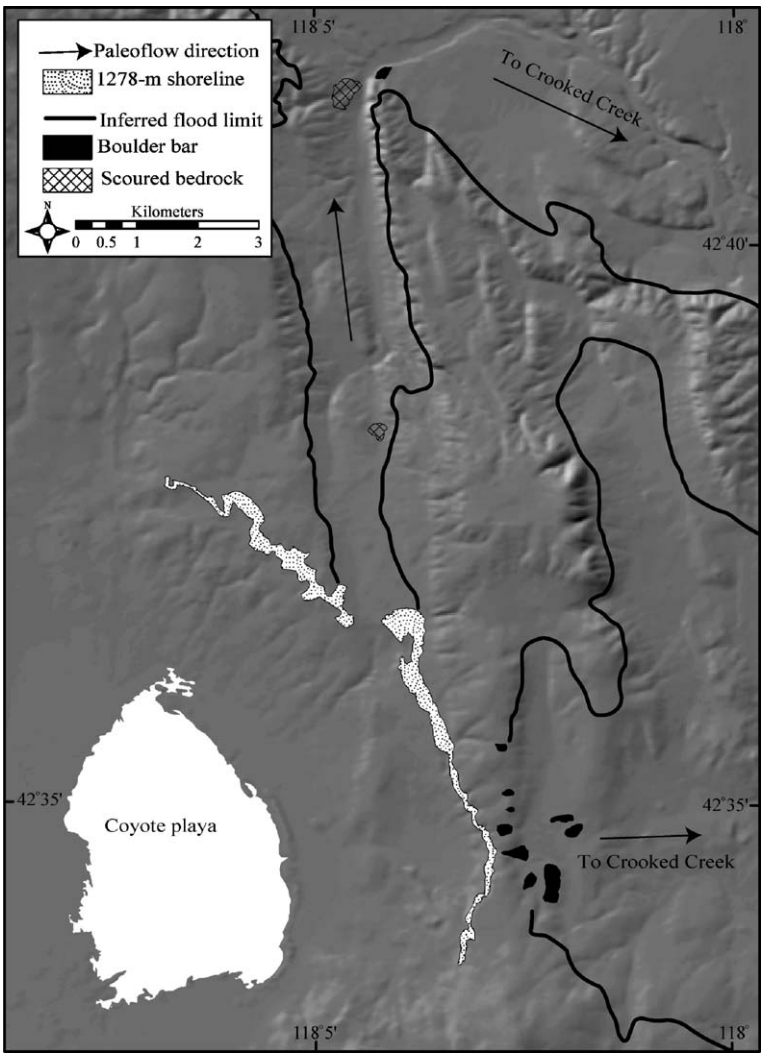

Fig. 6. Geomorphic map of the northern and eastern outlets of Lake Coyote.

nificantly older than the 1278-m shoreline in Coyote Basin (Fig. 4) and the 1280- and 1292-m shorelines in Alvord Basin for the following reasons: (1) It is discontinuous throughout Coyote Basin, which could result from either greater age or shorter lake duration at this level. (2) Rounded clasts forming the shoreline features have continuous carbonate coatings (stage II+) and are darkly varnished and polished in contrast to clasts on the 1278-m shoreline. (3) Shallow excavation (<50 cm) into the 1292-m shoreline revealed a thick Av horizon and a well-developed argillic horizon.

The 1278-m altitude of the lower, more prominent, shoreline matches the altitude of two divides separating Coyote Basin from Crooked Creek drainage to the east. Apparently, Lake Coyote, like Lake Alvord, was maintained at this stage for an extended period by overflow. The northern outlet is a 3-km wide saddle (now covered with eolian sand) leading to an 8-km long channel that heads north then east (Fig. 6). The eastern divide is a broad saddle approximately 4 km wide, containing five distinct bedrock swales at elevations ranging from 1278 to 1292 m. The floors of each of these bedrock swales, except the 1292-m swale, are littered with subrounded basaltic boulders and cobbles up to 20 cm in intermediate-axis diameter. The 1292-m swale is blanketed by eolian sand. The 1278-m swale grades downstream (eastward) to a large gravel fan.

4.5. The lake and overflow sequence

Taken together, the geomorphic and geochronologic evidence points to the following sequence of events

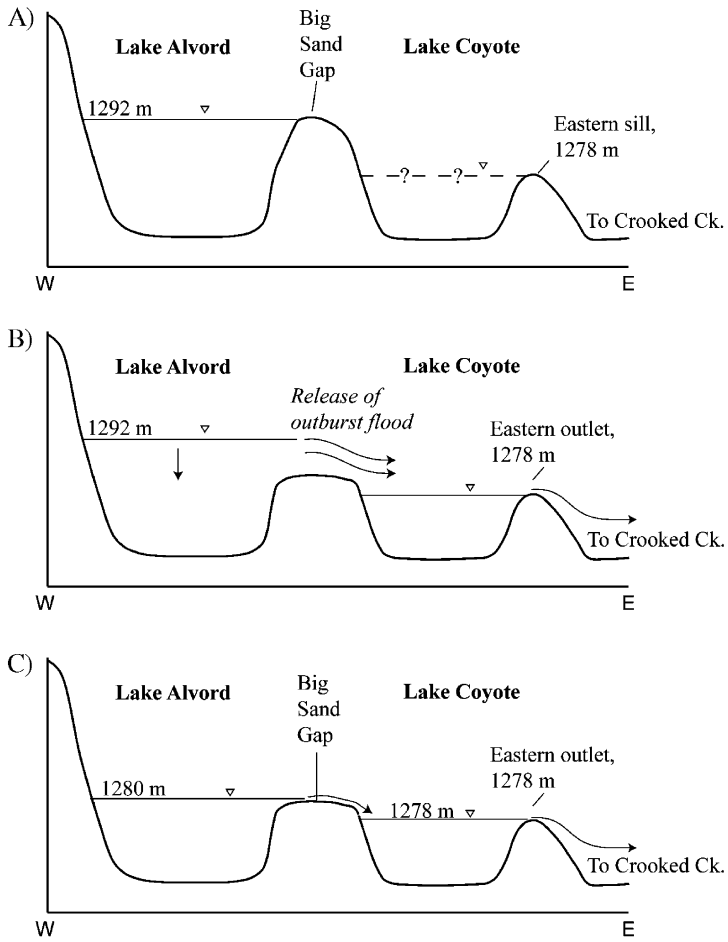

Fig. 7. Schematic illustration of the most recent late Pleistocene catastrophic draining of Lake Alvord related to a 1292- to 1280-m drop. (A) Lake Alvord is dammed by Big Sand Gap at 1292 m. If Lake Coyote contained a lake at this time, it would have been held in by a sill at 1278 m. (B) Lake Alvord briefly rises above 1292 m and initiates rapid incision at Big Sand Gap, releasing a catastrophic outburst flood into the Lake Coyote Basin. Overflow would have traveled through pre-existing Lake Coyote outlets at 1278 m and into Crooked Creek drainage. (C) Following the outburst flood, both lakes formed a nearly continuous water body at ~1280 m for an extended period.

(Fig. 7). During the late Pleistocene, sometime before ca. 13 ka (^{14}C yr), Lake Alvord stabilized at an elevation of 1292 m, with its outlet controlled by coarse alluvium or bedrock in the floor of Big Sand Gap. After sufficient time to develop the prominent 1292-m shoreline, incision at Big Sand Gap dropped the lake level to 1280 m. This 12 m of incision of Big Sand Gap may have been abrupt, only halting when resistant bedrock was encountered at 1280 m, or it may have been episodic, first dropping Lake Alvord from 1292 m to 1287 m for a short period so as to form the 1287-m shoreline preserved at Miranda Flat, and then dropped to 1280 m. In either case, Lake Alvord remained at 1280 m for sufficient duration to build and etch the prominent 1280-m Lake Alvord shoreline features. Initial overflow at the 1292-m level would have filled Coyote Basin to the level of the two 1278-m outlets leading to Crooked Creek (Fig. 5). As suggested by Lindberg and Hemphill-Haley (1988), Hemphill-Haley et al. (1999), and Lindberg (1999), the prominence of late-Pleistocene shoreline features in Alvord and Coyote Basins indicates prolonged late-Pleistocene overflow from Alvord Basin into Crooked Creek, and downstream into the Owyhee and Snake Rivers.

The older Alvord and Coyote Basin shorelines may indicate earlier periods of overflow into Crooked Creek, although the evidence is much less complete and altitudes may have been altered by tectonic displacement. The high, older shoreline at 1310 m in Alvord Basin, as well as the 1292-m shoreline in Coyote Basin, may indicate a breach in Big Sand Gap involving a Lake Alvord drop from 1310 m to as low as 1292 m, which is consistent with the range of bedrock swale altitudes on the eastern divide of the Coyote Basin. A possible scenario is that spillover from Lake Alvord raised the level of Lake Coyote to 1292 m long enough to form a shoreline at this altitude. Overflow of Coyote Basin at this elevation then eroded highest-altitude outlet channels in the eastern divide of Coyote Basin to the present-day elevation of 1278 m. This scenario, however, requires that the level of the northern divide in Coyote Basin was also at an altitude of at least 1292 m at this time, and later somehow lowered to its present elevation of 1278 m. Such lowering may have resulted from (1) tectonic displacement in the northern divide that may be evident in the linear, north–south drainage originating from the divide (Fig. 6); and/or (2) erosion of the northern divide from 1292 m to 1278 m contemporaneous with erosion of the eastern outlet. Neither of these explanations is very satisfying and we remain mystified by the evidence for a 1292-m lake in a basin that now has two widely separated outlets at the exact same elevation of 1278 m.

5. Geologic evidence of downstream flooding

On the basis of downstream flood evidence first noted by Marith Reheis and Mark Hemphill-Haley (Hemphill-Haley et al., 1999), one or more of these outflows from pluvial Lake Alvord was cataclysmic, sending a large volume of water into Crooked Creek drainage. The most likely scenario for a large flood from pluvial Lake Alvord is that resulting from rapid erosion of Big Sand Gap from 1292 m to 1280 m. Such erosion would have abruptly released 11.3 km^3 of water into Coyote Basin (presumably already full with water from sustained overflow from the 1292-m level of Lake Alvord) which would in turn enter Crooked Creek drainage via the two 1278-m outlets on the eastern and northern margins of the basin.

Downstream of both Coyote Basin outlets, scabland terrain and boulder bars are evidence for at least one significant flood flowing 59 km to the Owyhee River, mainly following the Crooked Creek drainage (Fig. 8). The maximum stage of flooding was defined by mapping the upper limits of flood deposits, eroded topography, and crossed and uncrossed divides using methods described by O'Connor (1993). Water-surface elevations were interpolated along the entire flood route using hydraulic modeling.

The northern and eastern outlets of Coyote Basin show evidence of substantial overflow. Overflow from the northern outlet traveled down a northward-trending channel, scouring bedrock and forming a large pendant boulder bar at a channel expansion 8 km downstream of the outlet (Fig. 6). Downstream from the eastern divide are large boulder bars (in addition to the gravel fan formed directly downstream of the 1278-m outlet). The flood paths from the northern and eastern outlets converged near the modern headwaters of Crooked Creek, west of U.S. Highway 95 (Fig. 8).

Downstream of the convergence of the two separate outlet routes, the flood eroded and enlarged canyons, stripped basaltic bedrock surfaces, and deposited large boulder and gravel bars, some of which are over 30 m above the present-day Crooked Creek channel (Fig. 8). Such flood features were observed throughout Crooked Creek drainage and are described in the Appendix. The most notable erosional features related to flooding are deeply incised bedrock canyons with stripped and scoured bedrock surfaces and scabland topography. One example is Well Canyon, which may have been entirely incised by the outburst flood. Well Canyon is a

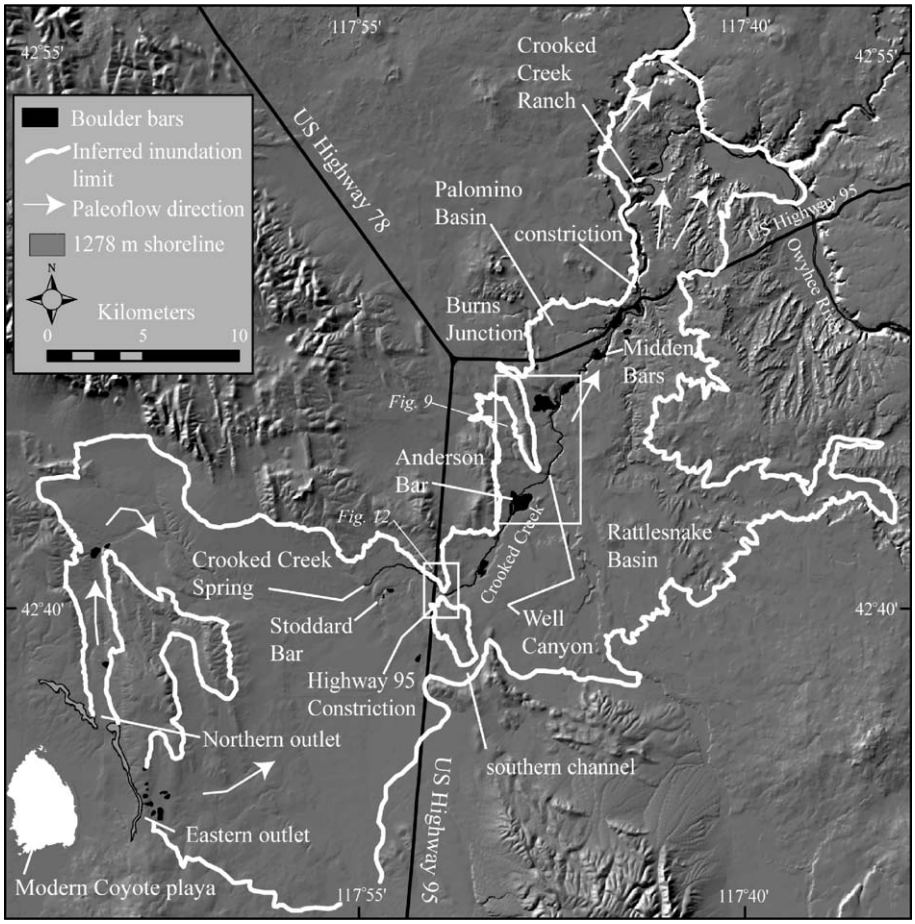

Fig. 8. Inundation limit and route of flooding along Crooked Creek. Inundation limit is based on surveyed geologic evidence and water-surface elevations generated from hydraulic modeling. All geologic evidence of flooding is listed in the Appendix. Boxes indicate locations of Figs. 8 and 12.

20-m deep gorge bisecting a northwest-trending bedrock ridge (Fig. 9). Upstream of Well Canyon, the modern Crooked Creek flows through the low-gradient Rattlesnake Creek basin before entering the canyon (Fig. 8). Rounded boulder bars lie above the western rim of Well Canyon, 30 m above present-day Crooked Creek. Numerous rounded cobbles and pebbles occur among the angular talus colluvium on the face of the ridge, and large boulder bars have formed downstream of the canyon. Two large bedrock "scabs" are present near the confluence of Crooked Creek and Owyhee River at Crooked Creek Ranch (Fig. 8), in the form of isolated bedrock knobs that lie along the path of Crooked Creek, and are mantled with rounded basaltic boulders and cobbles.

Notable depositional features along the flood route include large boulder bars, some of which were previously noted by other researchers (Hemphill-Haley et al., 1999; Marith Reheis, U.S. Geological Survey, personal communication, 2003). Most boulder bars are downstream of incised bedrock canyons and are composed of rock types found in the walls of the upstream canyons. Stoddard Bar, upstream of the Highway 95 Constriction, is a teardrop-shaped bar with angular–subangular imbricated boulders up to 1.5 m in intermediate diameter (Fig. 10). The Midden Bars are three boulder terraces that contain subangular to subrounded boulders in a matrix of rounded to subrounded cobbles and gravels (Fig. 10). The boulders have intermediate diameters up to 1 m and some are imbricated in the direction of flow. Anderson Bar is a large expansion bar downstream of an incised bedrock canyon and contains the largest boulders observed along the flood route; some with intermediate diameters as large to 4.1 m. The Anderson Bar boulders are strongly imbricated (Fig. 10).

The distribution of erosional and depositional features reflects the water-surface profile of the flood(s)

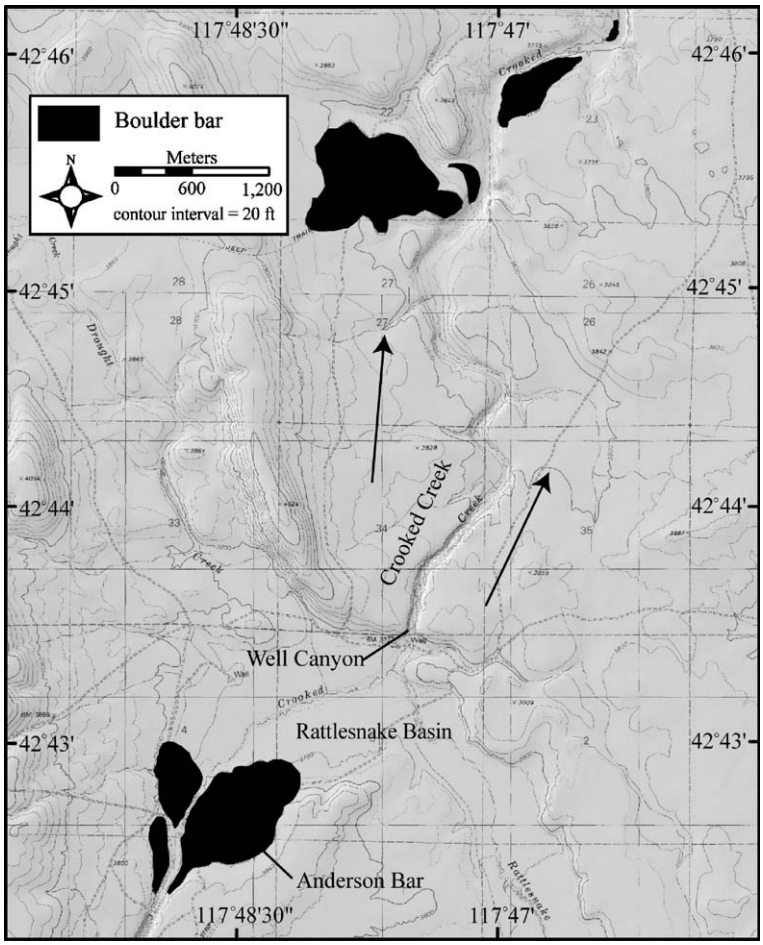

Fig. 9. Geomorphic map of Well Canyon vicinity. The modern canyon of Crooked Creek is deeply incised into bedrock in this reach; it was likely eroded through flooding.

and indicates that the flow gradient generally followed the slope of Crooked Creek (Fig. 11). In detail, however, flood profiles consisted of short high-gradient reaches within constrictions separated by longer low-gradient reaches where the flow route was wider. Along the flood route, reaches with steep, narrow, channel geometries generally exhibit erosional features such as incised bedrock canyons and stripped bedrock surfaces, whereas reaches with wide, low-gradient geometries tend to contain depositional features, such as boulder and cobble bars.

Flood evidence lies directly upstream of the narrowest parts of Highway 95 Constriction and Well Canyon (Fig. 11), and probably reflects ponding above narrow channel constrictions that hydraulically dammed flow. It is plausible that some deposition occurred in topographically high positions during the initial stages of flooding, such as the upper terrace of the Midden Bars, and as flooding further entrenched pre-existing canyons, these upper deposits were abandoned, and new deposits were formed at lower levels in the enlarged canyons (Fig. 10). Alternatively, the highest-altitude deposits may have been emplaced by larger-magnitude floods, and the lower deposits may have been reworked by subsequent smaller floods.

5.1. Age of flood deposits

While the late-Pleistocene drop of pluvial Lake Alvord from 1292 m to 1280 m is the most obvious scenario to produce a large flood, we cannot yet rule out other scenarios. It is possible that older outburst floods occurred related to the 1310-m Lake Alvord level (Hemphill-Haley, 1987; Lindberg and Hemphill-Haley, 1988; Hemphill-Haley et al., 1999), although little evidence exists for the exact sequence and lake-level elevations. It is possible that multiple smaller late-Pleistocene floods occurred because of episodic

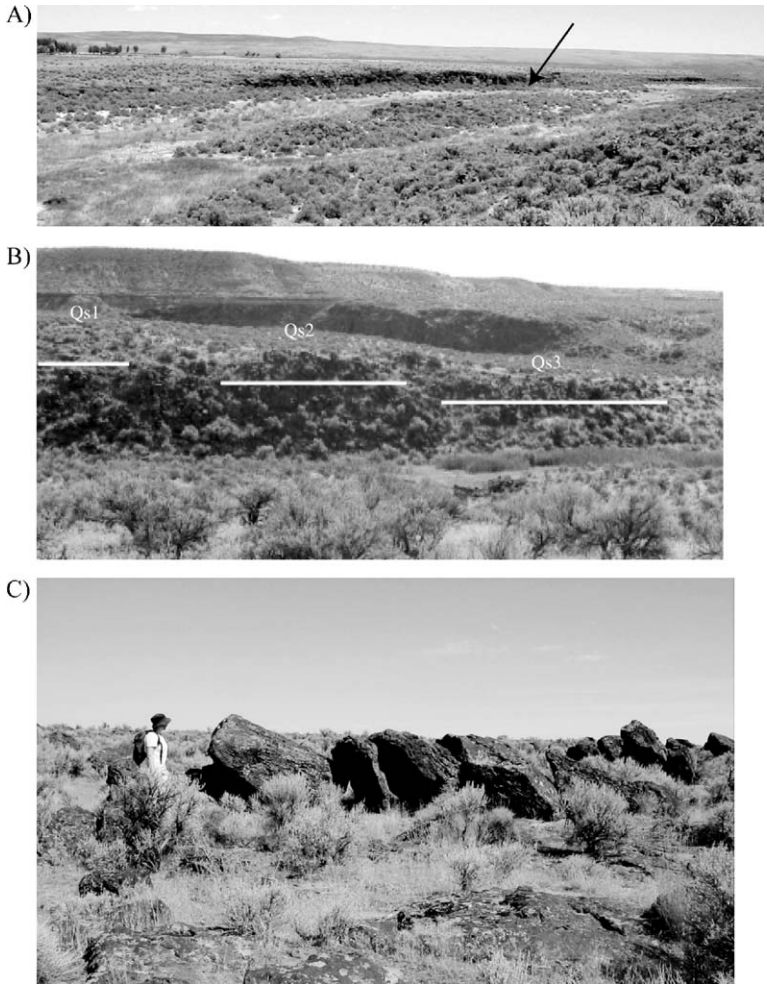

Fig. 10. Boulder bars along flood route. (A) Stoddard Bar (indicated by arrow) is teardrop-shaped with imbricated boulders as much as 1.5 m in intermediate axis diameter. Bar is approximately 160 m long. (B) The Midden Bars contain multiple surfaces of similar age (Qs1, Qs2, Qs3), based on relative dating. Boulders are imbricated, rounded, and <1 m in intermediate axis diameter. Qs1 and Qs2 may have become abandoned as flooding enlarged the canyon and flood stage dropped. Qs2 is approximately 70 m across. (C) Imbricated Anderson Bar boulders are up to 4.1 m in intermediate axis diameter.

lowering of Lake Alvord to 1280 m from its 1292-m highstand.

Direct dating of flood features using radiocarbon and ^{3}He cosmogenic geochronology has been largely unsuccessful so far. We found no material suitable for ^{14}C dating. Attempts at cosmogenic ^{3}He dating of olivine- and pyroxene-bearing basaltic boulders at Anderson and Midden Bars resulted in a wide range of ages (Table 3). Six boulders and two shielded samples from two flood bars were sampled. Four boulders and a shielded sample were collected from Anderson Bar (Fig. 8), and two boulders and a shielded sample were collected from Midden Bar (Fig. 8). The shielded samples were collected from underneath overhangs in basalt flows that likely provided the flood deposits. The shielded sample at Anderson Bar was collected 2.5 m below the surface of the flow and 1.5 m into the flow. The basalt flow was upstream of Anderson Bar and had no cover (e.g. flood deposits) on it. The shielded sample at Midden Bars was collected downstream of the Midden Bars and was >2 m below the surface of the flow and 35 cm into the flow. Samples were prepared and processed in accordance with Cerling and Craig (1994).

The surface ages derived from the flood boulders range from 171 ± 12 to 11 ± 1 ka; however, flood deposits sampled for ^{3}He cosmogenic dating had minimal rock varnish and shallow soil pits (>75 cm) revealed a weak Av horizon and stage I carbonate development, implying that these soils and deposits are likely late Pleistocene. The most probable explana-

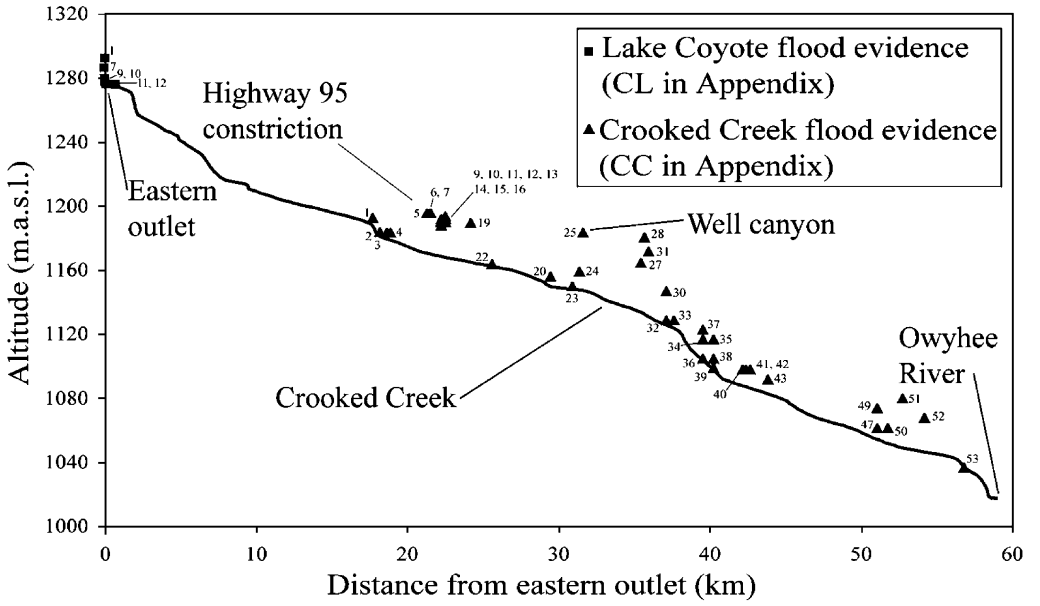

Fig. 11. Profile of flood route from the eastern outlet of Lake Coyote to the Owyhee River showing elevations of field evidence indicating minimum peak flood stage (labeled). Numbered flood features and locations are described in the Appendix. M.a.s.l.=meters above sea level.

tion for the wide range of cosmogenic ^{3}He ages is the accumulation of substantial amounts of noncosmogenic ^{3}He/^{4}He through radiogenic decay, as basalts near these sampling sites yield K–Ar ages of 7.87 ± 0.55 and 7.81 ± 0.55 Ma (Walker and Repenning, 1966; Fiebelkorn et al., 1983) which would allow sufficient time for the production of radiogenic ^{3}He/^{4}He. Noncosmogenic ^{3}He can be derived from primordial mantle gases, accumulated from the atmosphere, or produced from radiogenic decay of ^{6}Li (Andrews, 1985; Cerling and Craig, 1994). ^{4}He can be attributed to the decay of ^{238}U, ^{235}U, and ^{230}Th (Andrews, 1985). Long-term accumulation of radiogenic ^{3}He can be a significant contribution to total ^{3}He and overwhelm the cosmogenic ^{3}He accumulated within the surfaces of young (Holocene and late-Pleistocene) landforms (Cerling and Craig, 1994; Gosse and Phillips, 2001). Because cosmogenic ^{3}He dating relies on the relative ratio of ^{3}He/^{4}He, high levels of non-cosmogenic ^{3}He and ^{4}He also affect the accuracy of the ages.

Table 3
^{3}He exposure ages for Anderson and Midden Bars, Crooked Creek, Oregon

Sample	Latitude	Longitude	Elevation (m)	Mass (g)	R/R_a	^{4}He ± analytical error (10^{9} atoms/g)	^{3}He ± analytical error (10^{6} atoms/g)	^{3}He$_c$(%)	Production rate (atoms/g/yr)	Cosmogenic ^{3}He$_c$ age ± uncertainty (ka)
Anderson Bar										
073103-01	42.712	117.81	1154	0.1221	17.95	2141.67 ± 107.08	51.24 ± 2.56	93.0	298.85	171 ± 12
073103-02	42.712	117.81	1154	0.1033	7.49	4373.77 ± 218.69	38.76 ± 1.94	83.0	298.85	130 ± 9
073103-04	42.712	117.81	1154	0.1017	5.14	3041.65 ± 152.08	16.67 ± 0.83	75.7	298.85	56 ± 4
073103-05	42.712	117.81	1154	0.0744	2.99	3537.51 ± 176.88	8.45 ± 0.42	79.5	298.85	28 ± 2
Midden Bars										
080103-06	42.779	117.76	1121	0.0439	1.06	5247.88 ± 262.39	3.38 ± 0.17	42.2	298.77	11 ± 1
080103-08	42.781	117.76	1106	0.0648	0.60	5819.12 ± 290.56	–	–	298.85	–
Shielded samples										
042504-03	42.710	117.81		0.2368	1.33[a]	255.03 ± 12.75				
080103-10	42.712	117.81		0.1261	0.61[b]	2109.02 ± 105.45				

Sample 042504-03 analyzed at USGS Noble Gas Mass Spectrometer Lab, Denver, CO; all other samples analyzed at University of Utah Department of Geology and Geophysics Noble Gas Mass Spectrometer Lab, Salt Lake City, UT.

[a] R/R_a value from shielded sample was subtracted from R/R_a values for all Anderson Bar samples to correct for non-cosmogenic ^{3}He.

[b] R/R_a value from shielded sample was subtracted from R/R_a values for all Midden Bars samples to correct for non-cosmogenic ^{3}He.

Nevertheless, we tentatively infer, on the basis of limited weathering and soil development, that most of the large depositional features resulted from a latest-Pleistocene episode of flooding associated with lowering of Pluvial Lake Alvord from its 1292-m level to its 1280-m level. As the hydraulic analyses described in the next section indicate, however, some flood features along Crooked Creek may have been left by older and larger floods.

6. Hydraulic analysis

Reconstruction of late Pleistocene lake-level histories and the flood profile along Crooked Creek drainage allowed us to estimate peak-flood discharges at two key locations: through Big Sand Gap at the outlet to Lake Alvord, and in a constricted segment of Crooked Creek, downstream of where the two Coyote Basin outlets converge and near the U.S. Highway 95 crossing.

Step-backwater methods used in conjunction with geologic evidence of the minimum flood stage provided a means to evaluate flow conditions and calculate peak discharge values. The step-backwater technique has been widely applied in paleoflood studies of large cataclysmic floods (Jarrett and Malde, 1987; O'Connor and Baker, 1992; O'Connor, 1993; Rathburn, 1993), and is described in detail by O'Connor and Webb (1988). The Hydrologic Engineering Center's River Analysis System (HEC RAS) 3.1 computer program from the U.S. Army Corps of Engineers (Hydrologic Engineering Center, 2003) was used to model water-surface profiles of potential peak-flood stages. HEC RAS is a model of one-dimensional flow that computes energy-balanced water-surface profiles based on channel geometry and estimated coefficients of energy loss. Cross-sections that define channel geometry were measured from 7.5′ USGS topographic maps and flood evidence was measured with PPK GPS. The peak-flood discharge was determined by computing water-surface profiles for a range of discharges and determining which best fit the elevations of flood evidence. For all reaches, a hydraulic roughness coefficient of 0.03 was assigned for the flow within the main channel, and 0.05 for overbank areas. Contraction and expansion coefficients were 0.1 and 0.3, respectively, as recommended by HEC RAS.

6.1. Big Sand Gap and Coyote Basin outlets

Assuming that Lake Alvord was the source, the peak discharge of flooding is ultimately constrained by the rate that flow can exit via Big Sand Gap. Maximum flow is associated with the state of critical flow, which is the condition of maximum discharge for the available specific energy. For lake and reservoir releases, discharge is exponentially related to the drop of lake level, and, for cases where lake volume is small relative to lake drop, the time it takes the breach to fully develop (Walder and O'Connor, 1997). For the Lake Alvord situation, the volume of the lake is large relative to the lake drop, and simple critical flow estimates based on channel geometry and lake-level drops provide maximum limits of downstream flood discharge for given lake drainage scenarios.

For critical flow through the narrowest section of Big Sand Gap (Fig. 5), maximum outflow associated with an instantaneous drop in lake level from 1292 m to 1280 m is 8000 $m^3\ s^{-1}$. If we assume that Lake Alvord temporarily rose to ~1293 m so as to initiate breaching of the previously stable 1292-m outlet, the peak discharge could have been as great as 10,000 $m^3\ s^{-1}$. This 8000–10,000 $m^3\ s^{-1}$ range is an upper limit of peak discharge for the late-Pleistocene release from Lake Alvord and the downstream flood. For the corresponding flood volume of 11.3 km^3, the flood duration would be about 13 days at continuous discharge of 10,000 $m^3\ s^{-1}$; however, actual flood duration would have much longer (probably on the order of several weeks) because the discharge would have decreased significantly as the lake level dropped.

It is possible that older overflow events occurred at Big Sand Gap related to the 1310-m shoreline in Alvord Basin. Maximum peak discharge associated with a drop from 1310 m to the base of Big Sand Gap at 1280 m is 40,000 $m^3\ s^{-1}$. Maximum peak discharge associated with a 1310- to 1292-m drop is 22,000 $m^3\ s^{-1}$.

The two wide outlets of Lake Coyote easily conveyed maximum flows exiting Alvord Basin via the much narrower Big Sand Gap. The northern outlet could pass a maximum of 120,000 $m^3\ s^{-1}$ and the eastern outlet a maximum of 70,000 $m^3\ s^{-1}$ at critical flow for a temporarily flooded lake level of 1292 m. Water entering Coyote Basin at a rate of 10,000 $m^3\ s^{-1}$ through Big Sand Gap would only force Lake Coyote to rise ~2 m to pass the flow through its two outlets with their present geometry.

6.2. Highway 95 Constriction

The first constriction that confined the floodwaters from both outlets of Lake Coyote into a single channel appropriate for hydraulic modeling is where present-day Crooked Creek intersects U.S. Highway 95 (Fig. 8). Four channel cross-sections were measured from the

7.5′ USGS Anderson Reservoir topographic map and entered into the step-backwater model to calculate paleodischarge (Fig. 12). For this location, flow was calculated to be critical for all reasonable modeling conditions for the range of flows required to achieve stages as high as indicated by the upstream flood evidence.

The highest flood deposits at this site consist of subrounded boulders, cobbles and pebbles of lithologies different than the local bedrock, but equivalent to rock types upstream. These deposits indicate that flooding achieved a maximum stage of at least 1187–1191 m near the entrance to the constriction (Fig. 12). For present-day channel geometry, a discharge of 40,000 $m^3\ s^{-1}$ is required to produce a calculated water-surface profile that matches the elevation of this flood evidence (Fig. 13A).

Another divide lies 4.3 km south of the Highway 95 Constriction and shows no evidence that flooding crossed it (southern channel in Fig. 8). A transverse gravel bar (CC-5 in Appendix), however, lies on the upstream side of the divide at 1195 m, and provides evidence that flooding reached this altitude. A discharge of 40,000 $m^3\ s^{-1}$ generates a water-surface elevation that encompasses this bar but does not cross this southern divide.

This result of 40,000 $m^3\ s^{-1}$ for the Highway 95 Constriction is problematic in that it is about four times larger than the maximum possible late-Pleistocene outflow rate of Pluvial Lake Alvord. It is unlikely that the

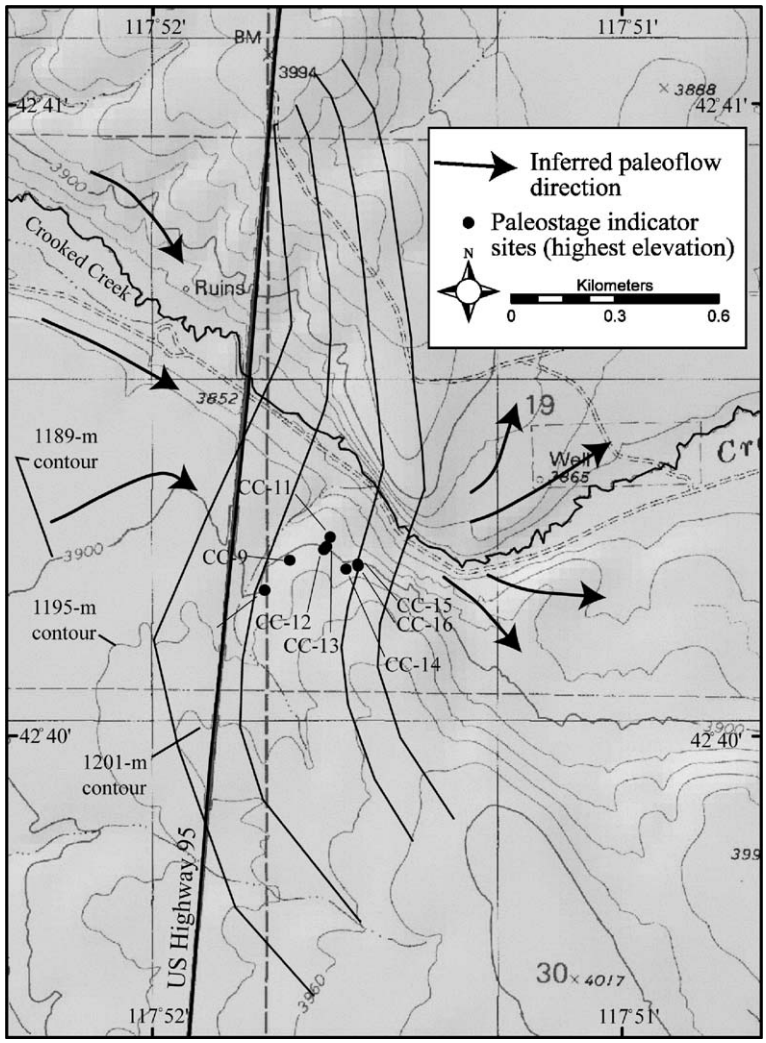

Fig. 12. Cross-section locations and surveyed paleostage indicators (PSIs) for Highway 95 Constriction. Surveyed PSIs indicated on the map represent the highest-elevation flood deposits; numerous rounded boulders and cobbles were observed at lower elevations within the constriction. Exact locations and altitudes of these PSIs are listed in the Appendix.

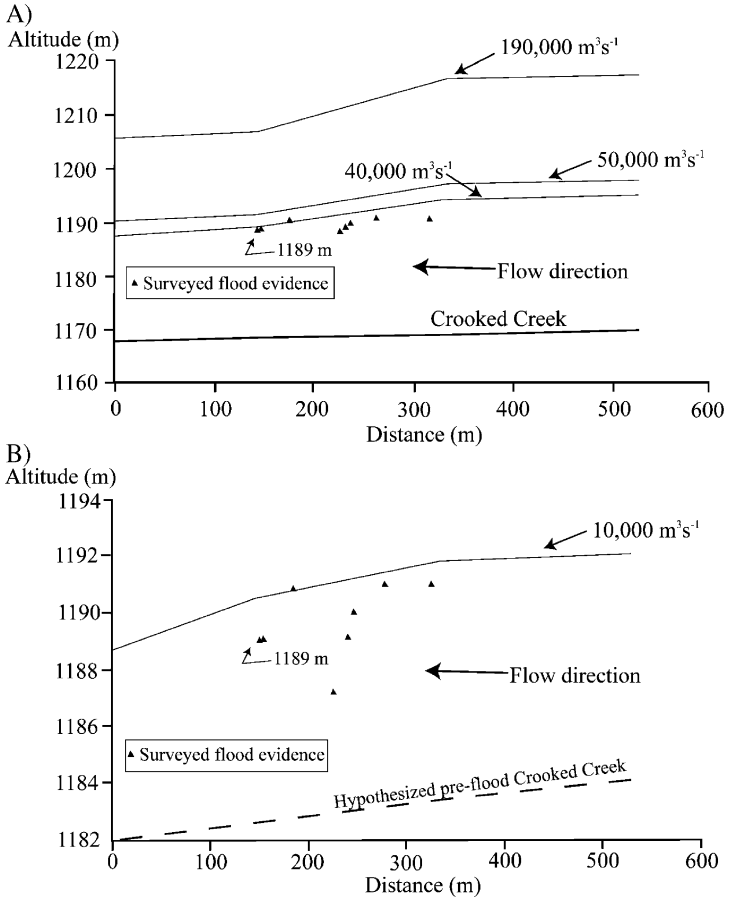

Fig. 13. Reconstructed water-surface profiles for Highway 95 Constriction (note different vertical scales). (A) Using modern channel geometry, a minimum peak discharge of 40,000 m^3 s^{-1} best matches surveyed flood evidence. Flows of 190,000 m^3 s^{-1} that could be generated by a breach of both Lake Coyote outlets produces a water surface well above the highest-elevation flood evidence. (B) If vertical incision of 13 m occurred during flooding, a minimum peak discharge of 10,000 m^3 s^{-1} is required to match flood evidence and to accord with modeled discharge at Big Sand Gap related to a 1292-m to 1280-m drop in elevation of Lake Alvord.

flow would have sufficient additions of either water or sediment to account for a four-fold increase in peak discharge. Other possibilities for the discrepancy are: (1) the Highway 95 constriction was greatly enlarged during the course of a 10,000 m^3 s^{-1} flood, hence giving a larger discharge calculated on the basis of present geometry; (2) multiple floods carved the bedrock canyons and produced some incision during each event; or (3) flood deposits and crossed drainage divides observed along Crooked Creek drainage were produced by an earlier flood of 40,000 m^3 s^{-1} followed by the 10,000 m^3 s^{-1} latest-Pleistocene outburst.

In consideration of scenario 1, about 13 m of canyon incision during the flood would allow a peak flood discharge of 10,000 m^3 s^{-1} (early in the flood) to leave the highest observed flood evidence at the Highway 95 Constriction (Fig. 13B). The incised bedrock canyons observed upstream of Stoddard and Anderson bars and at Well Canyon do provide strong evidence that at least one flood along Crooked Creek caused substantial erosion, which would have steepened the channel and lowered the local base level for the Highway 95 Constriction reach a few kilometers upstream.

We further assessed the plausibility of such erosion by consideration of flow stream power, which is a measure of the amount of work done by the flow on the landscape and is proportional to the product of energy gradient, fluid density, and flow velocity. The maximum mean stream power calculated for a discharge of 10,000 m^3 s^{-1} at the Highway 95 Constriction is 2360 Wm^{-2}. This value is within range of stream power values associated with basalt erosion for the Big Lost River Flood in Idaho (Rathburn, 1993; 600–5000 Wm^{-2}) as well as for the Bonneville Flood (O'Connor, 1993; 300–30,000 W m^{-2}). It is, however, unclear whether one flood event could accomplish 13 m

of incision at the Highway 95 Constriction given the relatively short duration calculated for an outburst flood of 10,000 $m^3 s^{-1}$ to lower Lake Alvord from the 1292- to 1280-m shorelines.

Evidence in Alvord and Coyote Basins indicates that both held older and higher lakes, which could presumably produce larger outburst floods. Plausible scenarios include (1) a drop in Lake Alvord from the highest shoreline at 1310 m to one of the lower shorelines at either 1292 or 1280 m, or (2) a catastrophic breach of the outlets of Lake Coyote from a stage of 1292 m or higher. Step-backwater calculations indicate that a flood resulting from a 1310- to 1280-m drop in Lake Alvord would discharge ~40,000 $m^3 s^{-1}$ through Big Sand Gap, similar to the calculated discharge for the highest observed flood deposits at the Highway 95 Constriction. In this scenario, the highest-altitude paleostage indicators observed along Crooked Creek would have been deposited by an older flow of 40,000 $m^3 s^{-1}$. The lower-altitude deposits could represent deposits left by the late-Pleistocene 10,000 $m^3 s^{-1}$ flood associated with a 1292- to 1280-m drop in Lake Alvord.

Another but less likely scenario could be a rapid release from Coyote Basin. The older 1292-m shoreline and channels up to 1292 m in the eastern divide of Coyote Basin illustrate that it held an older lake that overflowed after reaching this altitude. A breach of a full Lake Coyote, perhaps caused by the overflow from Lake Alvord, could generate an initial flood burst as great as 190,000 $m^3 s^{-1}$ if the northern and eastern outlets simultaneously discharged at critical flow. A discharge of this magnitude would create a water-surface well above even the highest flood evidence observed along Crooked Creek (Fig. 13A). Release of a flood of this magnitude, however, would require simultaneous incision of both outlets of Lake Coyote from 1292 m to 1278 m, which seems implausible without a much larger inflow into the basin. Outflow from a single Coyote Basin outlet could produce a discharge of 70,000 (eastern outlet) to 120,000 (northern outlet) $m^3 s^{-1}$, but such scenarios require explanation of the later development of the other outlet to the same elevation.

The cause of the 40,000 $m^3 s^{-1}$ discharge at the Highway 95 Constriction is unresolved. Barring misinterpretation of high-water evidence, it seems that this large discharge most likely resulted from an earlier Pleistocene overflow of Pluvial Lake Alvord, because the latest Pleistocene conditions apparently only permit a maximum discharge 10,000 $m^3 s^{-1}$. Judging from weathering characteristics, most of the downstream flood deposits probably resulted from this 10,000 $m^3 s^{-1}$ flood.

7. Conclusions

Overflow of pluvial Lake Alvord and downcutting at Big Sand Gap released a large outburst flood into Crooked Creek drainage and into the Owyhee River. Surficial characteristics of shorelines and the presence of diatoms in Lake Alvord sediment indicative of deep, open-basin conditions at about the time of Mt. St. Helens set Sg tephra deposition suggest that initial spilling from the 1292-m Lake Alvord level was before ~13–14 ka (^{14}C yr) and that the flood may have been at about this time. Older shoreline features indicate the existence of earlier, higher lakes in both Alvord and Coyote Basins, but overflow conditions are not fully known. The geometry at Big Sand Gap limited the maximum peak discharge of the late-Pleistocene flow due to a 1292- to 1280-m drop in Lake Alvord to about 10,000 $m^3 s^{-1}$. This discharge is consistent with much of the evidence for erosion and deposition along Crooked Creek drainage to the Owyhee River; however, hydraulic modeling results in conjunction with maximum flood stage evidence require a minimum peak discharge of ~40,000 $m^3 s^{-1}$ for the present geometry at the Highway 95 Constriction. This much larger value perhaps results from significant erosion of the constriction during the late-Pleistocene 10,000 $m^3 s^{-1}$ flood, or to an older, larger flood from overflow of either the Alvord or Coyote Basins.

Prominent shorelines at 1292 and 1280 m in Alvord Basin and 1278 m in Coyote Basin require sustained lake levels at those altitudes before and after erosion of the outlet and Big Sand Gap, indicating persistent overflow of the Lake Alvord system into Crooked Creek and the Owyhee River. This outflow would have provided a surface drainage connection between the northernmost Great Basin and the Columbia River drainage basin for an extended period before and after the late-Pleistocene outburst flood down Crooked Creek.

The magnitude of the most recent Crooked Creek flood falls between relatively frequent meteorological floods that are typically confined to existing canyons and floodplains, and the rare megafloods that transform landscapes on immense scales, such as the Missoula Floods. Although the magnitude of the most recent Crooked Creek flood did not approach that of the largest late-Pleistocene floods, it significantly altered the landscape of its watershed by eroding deep canyons, depositing large boulder bars, and altering drainage-basin connections. These changes attest to the significant effects of intermediate scale, nonmeteorological floods on landscape evolution.

Acknowledgments

This work is part of Carter's M.S. thesis for the Department of Geological Sciences at Central Washington University. We appreciate the assistance of Marith Reheis (USGS) who provided the initial inspiration for the project and much support throughout. We also thank Thure Cerling for use of the noble gas mass spectrometer at University of Utah, Scott Starratt (USGS) for diatom identification, and Nick Foit (Washington State University) for tephra analyses and identification. Thanks also to the faculty, staff, and students of the Department of Geological Sciences at Central Washington University. Funding was provided by NSF Grant EAR-9725336, a Jonathon O. Davis Scholarship, Sigma Xi Scientific Research Society, University of Washington Chapter of Sigma Xi, Geological Society of America, and Central Washington University Office of Graduate Studies. Stephen Slaughter, Erin Chamberlain, Steve Edwards, Erica Henry, Natalie Sudman, John Leistner, Jeff Peters, and Cooper Brossy assisted with field work. The project benefited from comments and discussions from Karl Lillquist and Scott Thomas, and Marc Fairbanks provided assistance with GIS. Marith Reheis, P. Kyle House, J. Michael Daniels, and Mark Hemphill-Haley provided thoughtful reviews that improved an earlier version of the manuscript.

Appendix A. Geologic evidence of flooding

No.	USGS quadrangle	Latitude[a]	Longitude[a]	Minimum altitude (ft)[b]	Maximum altitude (ft)[b]	Minimum altitude (m)[b]	Maximum altitude (m)[b]	Method of determining altitude[c]	Upper/ lower limit[d]	Feature
CL-1	Coyote Lk. East	42.590	118.049	4241	4249	1293	1295	Topography	L	Channelized boulders
CL-2	Coyote Lk. East	42.601	118.048	4283	4283	1305	1305	Spot elevation	U	Uncrossed divide
CL-3	Grassy Rdg. Well	42.626	118.080	4181	4189	1274	1277	Topography	L	Channelized boulders
CL-4	Grassy Rdg. Well	42.689	118.080	4120	4090	1256	1247	Topography	L	Scoured bedrock
CL-5	Grassy Rdg. Well	42.692	118.071	4081	4089	1244	1246	Topography	L	Pendant Bar
CL-6	Coyote Lk. East	42.581	118.045	4241	4249	1293	1295	Topography	L	Channelized boulders
CL-7	Coyote Lk. East	42.581	118.045	4221	4229	1286	1289	Topography	L	Channelized boulders
CL-8	Coyote Lk. East	42.578	118.046	4221	4229	1286	1289	Topography	L	Channelized boulders
CL-9	Coyote Lk. East	42.575	118.044	4192	4192	1278	1278	Spot Elevation	L	Channelized boulders
CL-10	Coyote Lk. East	42.576	118.047	4201	4209	1280	1283	Topography	L	Channelized boulders
CL-11	Coyote Lk. East	42.570	118.041	4181	4189	1274	1277	Topography	L	Boulder bar
CL-12	Coyote Lk. East	42.570	118.037	4181	4189	1274	1277	Topography	L	Boulder bar
CL-13	Coyote Lk. East	42.586	118.033	4181	4189	1274	1277	Topography	L	Boulder bar
CL-14	Coyote Lk. East	42.580	118.034	4181	4189	1274	1277	Topography	L	Boulder bar
CC-1	Flat Top Mtn.	42.670	117.879	3901	3919	1189	1194	Topography	L	Scour
CC-2	Flat Top Mtn.	42.670	117.897	3901	3919	1189	1194	Topography	L	Boulder bar
CC-3	Flat Top Mtn.	42.670	117.888	3891	3899	1186	1188	Topography	L	Boulder bar
CC-4	Flat Top Mtn.	42.674	117.893	3881	3889	1183	1185	Topography	L	Boulder bar
CC-5	Anderson Res.	42.645	117.873	3920	3939	1195	1201	Topography	L	Gravel bar
CC-6	Anderson Res.	42.508	117.868	3914	3919	1193	1194	Survey	L	Boulders
CC-7	Anderson Res.	42.649	117.868	3921	3939	1195	1201	Topography	L	Boulders
CC-8	Anderson Res.	42.646	117.859	3923	3923	1196	1196	Spot elevation	L	Boulders
CC-9	Anderson Res.	42.671	117.862	3908	3908	1191	1191	Survey	L	Boulder
CC-10	Anderson Res.	42.671	117.863	3908	3908	1191	1191	Survey	L	Pebbles
CC-11	Anderson Res.	42.672	117.860	3895	3895	1187	1187	Survey	L	Boulder
CC-12	Anderson Res.	42.672	117.860	3901	3901	1189	1189	Survey	L	Pebbles
CC-13	Anderson Res	42.672	117.860	3904	3904	1190	1190	Survey	L	Pebbles
CC-14	Anderson Res.	42.671	117.860	3908	3908	1191	1191	Survey	L	Pebbles
CC-15	Anderson Res.	42.671	117.859	3901	3901	1189	1189	Survey	L	Pebbles
CC-16	Anderson Res.	42.671	117.859	3901	3901	1189	1189	Survey	L	Pebbles
CC-17	Anderson Res.	42.658	117.849	4017	4017	1224	1224	Spot elevation	U	Uncrossed divide
CC-18	Anderson Res.	42.683	117.862	3991	3999	1216	1219	Spot elevation	U	Uncrossed divide
CC-19	Anderson Res.	42.650	117.827	3901	3919	1189	1194	Remote sensing	L	Possible cataract
CC-20	Anderson Res.	42.712	117.813	3791	3799	1155	1158	Topography	L	Boulder bar
CC-21	Anderson Res.	42.716	117.811	3781	3799	1152	1158	Topography	L	Boulder bar
CC-22	Anderson Res.	42.710	117.814	3801	3819	1158	1164	Topography	L	Plucked basalt
CC-23	Anderson Res.	42.722	117.795	3770	3779	1149	1152	Topography	L	Silts

(continued on next page)

Appendix A (*continued*)

No.	USGS quadrangle	Latitude[a]	Longitude[a]	Minimum altitude (ft)[b]	Maximum altitude (ft)[b]	Minimum altitude (m)[b]	Maximum altitude (m)[b]	Method of determining altitude[c]	Upper/ lower limit[d]	Feature
CC-24	Anderson Res.	42.726	117.792	3781	3799	1152	1158	Topography	L	Pebbles
CC-25	Anderson Res.	42.728	117.799	3881	3999	1183	1219	Topography	L	Boulders
CC-26	Anderson Res.	42.733	117.804	4024	4024	1226	1226	Spot elevation	U	Uncrossed divide
CC-27	Burns Jct.	42.757	117.794	3818	3818	1164	1164	Spot elevation	L	Boulder bar
CC-28	Burns Jct.	42.766	117.794	3872	3872	1180	1180	Survey	L	Gravel
CC-29	Burns Jct.	42.773	117.804	3781	3799	1152	1158	Topography	L	Pebbles
CC-30	Burns Jct.	42.783	117.801	3761	3779	1146	1152	Topography	L	Pebbles
CC-31	Burns Jct.	42.763	117.788	3842	3842	1171	1171	Survey	L	Abandoned channel
CC-32	Burns Jct.	42.766	117.781	3701	3719	1128	1133	Topography	L	Boulder bar
CC-33	Burns Jct.	42.769	117.772	3701	3719	1128	1133	Topography	L	Boulder bar
CC-34	Burns Jct.	42.771	117.766	3661	3679	1116	1121	Topography	L	Boulder bar
CC-35	Burns Jct.	42.780	117.757	3661	3679	1116	1121	Topography	L	Boulder bar
CC-36	Burns Jct.	42.780	117.759	3621	3639	1104	1109	Topography	L	Boulder bar
CC-37	Burns Jct.	42.779	117.763	3681	3699	1122	1127	Topography	L	Boulder bar
CC-38	Burns Jct.	42.781	117.762	3621	3639	1104	1109	Topography	L	Boulder bar
CC-39	Burns Jct.	42.794	117.747	3601	3619	1098	1103	Topography	L	Boulder bar
CC-40	Rome	42.785	117.741	3601	3619	1098	1103	Topography	L	Boulder bar
CC-41	Rome	42.785	117.742	3601	3619	1098	1103	Topography	L	Boulder bar
CC-42	Rome	42.798	117.747	3601	3619	1098	1103	Topography	L	Boulder bar
CC-43	Rome	42.800	117.737	3581	3599	1091	1097	Topography	L	Boulder bar
CC-44	Rome	42.800	117.735	3581	3599	1091	1097	Topography	L	Boulder bar
CC-45	Rome	42.802	117.681	3895	3895	1187	1187	Spot elevation	U	Uncrossed divide
CC-46	Rome	42.847	117.707	3641	3641	1110	1110	Spot elevation	L	Cobble
CC-47	Rome	42.848	117.734	3481	3499	1061	1066	Topography	L	Boulder bar
CC-48	Rome	42.853	117.734	3541	3559	1079	1085	Topography	L	Boulder bar
CC-49	Rome	42.852	117.731	3521	3526	1073	1075	Spot elevation	L	Abandoned water gap
CC-50	Rome	42.851	117.727	3461	3479	1055	1060	Topography	L	Boulder bar
CC-51	Rome	42.858	117.732	3541	3559	1079	1085	Topography	L	Cobble/abandoned water gap
CC-52	Rome	42.864	117.725	3501	3519	1067	1073	Topography	L	Boulder bar
CC-53	Owyhee Butte	42.864	117.716	3400	3419	1036	1042	Topography	L	Knickpoint/stripped bedrock
CC-55	Owyhee Butte	42.866	117.652	3381	3399	1030	1036	Topography	L	Boulders

[a] Latitude and longitude is listed in WGS-84 datum.

[b] Minimum and maximum elevations are given for each feature because of the uncertainty in determining the exact altitude of each feature. Uncertainty depends on the method used to locate the feature.

[c] Topography = altitude of feature by location with handheld GPS and location on USGS topographic maps; spot elevation = feature at or near the same altitude as a labeled altitude on a USGS map or near a surveyed benchmark; survey = feature altitude surveyed with Trimble PPK GPS or tape and clinometer; remote sensing = feature located on a aerial photo and/or topographic map.

[d] U = feature represents maximum flood limit because the feature was not inundated by the flood; L = feature represents a minimum flood limit.

References

Adams, K.D., 1997. Late Quaternary pluvial history, isostatic rebound, and active faulting in the Lake Lahontan basin, Nevada and California. Ph.D. Dissertation, University of Nevada, Reno, NV. 169 pp.

Adams, K.D., Wesnousky, S.G., 1998. Shoreline processes and the age of the Lake Lahontan Highstand in the Jessup embayment, Nevada. Geological Society of America Bulletin 110, 1318–1332.

Adams, K.D., Wesnousky, S.G., 1999. The Lake Lahontan highstand: age, surficial characteristics, soil development, and regional shoreline correlation. Geomorphology 30, 357–392.

Andrews, J.N., 1985. The isotopic composition of radiogenic helium and its use to study groundwater movement in confined aquifers. Chemical Geology 49, 339–351.

Baker, V.R., 1973. Paleohydrology and Sedimentology of Lake Missoula Flooding in Eastern Washington. Geological Society of America Special Paper, vol. 144. Boulder, CO. 73 pp.

Baker, V.R., Bunker, R.C., 1985. Cataclysmic late Pleistocene flooding from glacial Lake Missoula: a review. Quaternary Science Reviews 4, 1–41.

Beget, J.E., Keskinen, M.J., Severin, K.P., 1997. Tephrochronologic constraints of the late Pleistocene history of the southern margin of the Cordilleran ice sheet, western Washington. Quaternary Research 47, 140–146.

Behnke, R.J., 1992. Native Trout of Western North America. American Fisheries Society, Bethesda, MD. 275 pp.

Benito, G., O'Connor, J.E., 2003. Number and size of last-glacial Missoula floods in the Columbia River valley between the Pasco

Basin, Washington, and Portland Oregon. Geological Society of America Bulletin 115 (5), 624–638.
Berger, G.W., Busacca, A.J., 1995. Thermoluminescence dating of late Pleistocene loess and tephra from eastern Washington and southern Oregon and implications for the eruptive history of Mount St. Helens. Journal of Geophysical Research 100 (B11), 22,361–22,374.
Bretz, J.H., 1969. The Lake Missoula floods and the Channeled Scabland. Journal of Geology 77 (5), 505–543.
Cerling, T.E., Craig, H., 1994. Geomorphology and in-situ cosmogenic isotopes. Annual Review of Earth and Planetary Sciences 22, 273–317.
Clague, J.J., Barendregt, R., Enkin, R.J., Foit, F.F., 2003. Paleomagnetic and tephra evidence for tens of Missoula floods in southern Washington. Geology 31, 247–250.
Crandell, D.R., Mullineaux, D.R., Rubin, M., Spiker, E., Kelley, M.L., 1981. Radiocarbon dates from volcanic deposits at Mount St. Helens, Washington. U.S. Geological Survey Open-File Report 81-844, 1–15.
Fenton, C.R., Webb, R.H., Cerling, T.E., 2003. Peak discharge estimates of a Pleistocene lava-dam outburst flood, western Grand Canyon, Arizona, USA. Geological Society of America Abstracts with Programs 35 (6), 24.
Fiebelkorn, R.B., Walker, G.W., MacLeod, N.S., McKee, E.H., Smith, J.G., 1983. Index to K–Ar determinations for the state of Oregon. Isochron West 27, 3–60.
Freidel, D.E. 1993. Chronology and climatic controls of late Quaternary lake-level fluctuations in Chewaucan, Fort Rock, and Alkali basins, south-central Oregon. Ph.D. dissertation, University of Oregon, Eugene, OR. 244 pp.
Gosse, J.C., Phillips, F.M., 2001. Terrestrial in situ cosmogenic nuclides: theory and application. Quaternary Science Reviews 20, 1475–1560.
Hemphill-Haley, M.A., 1987. Quaternary stratigraphy and late Holocene faulting along the base of the eastern escarpment of Steens Mountain, southeastern Oregon. M.S. Thesis, Humboldt State University, Arcata, CA. 87 pp.
Hemphill-Haley, M.A., Page, W.D., Burke, R., Carver, G.A., 1989. Holocene activity of the Alvord fault, Steens Mountain, southeastern Oregon. Woodward-Clyde Consultant's Final Report to the U.S. Geological Survey Grant No. 14-08-0001-G1333, Oakland, CA. 45 pp.
Hemphill-Haley, M.A., Lindberg, D.A., Reheis, M.R., 1999. Lake Alvord and Lake Coyote: a hypothesized flood. In: Narwold, C. (Ed.), Quaternary Geology of the Northern Quinn River and Alvord Valleys, Southeastern Oregon, 1999 Friends of the Pleistocene Pacific Cell Field Trip Guidebook. Humboldt State University, Arcata, CA, pp. A21–A27.
Hubbs, C.L., Miller, R.R., 1948. The Zoological Evidence: correlation between fish distribution and hydrographic history. The Desert Basins of the Western United States, The Great Basin with Emphasis on Glacial and Postglacial Times. University of Utah, Salt Lake City, UT, pp. 18–144.
Hydrologic Engineering Center, 2003. HEC RAS User's Manual. U.S. Army Corps of Engineers, Davis, CA. 87 pp.
Jarrett, R.D., Malde, H.E., 1987. Paleodischarge of the late Pleistocene Bonneville Flood, Snake River, Idaho, computed from new evidence. Geological Society of America Bulletin 99, 127–134.
Knudsen, K.L., Sowers, J.M., Ostenna, D.A., Levish, D.R., 2002. Evaluation of glacial outburst flood hypothesis for the Big Lost River, Idaho. In: House, P.K., Webb, R.H., Baker, V.R., Levish, D.R. (Eds.), Ancient Floods, Modern Hazards; Principles and Applications of Paleoflood Hydrology. American Geophysical Union, Washington, DC, pp. 217–235.
Lindberg, D.N., 1999. A synopsis of late Pleistocene shorelines and faulting, Tule Springs Rims to Mickey Basin, Alvord Desert, Harney County, Oregon. In: Narwold, C. (Ed.), Quaternary Geology of the Northern Quinn River and Alvord Valleys, Southeastern Oregon. 1999 Friends of the Pleistocene Pacific Cell Field Trip Guidebook. Humboldt State University, Arcata, CA, pp. A3-1–A3-13.
Lindberg, D.N., Hemphill-Haley, M.A., 1988. Late-Pleistocene pluvial history of the Alvord Basin Harney Co., Oregon. Northwest Science 62 (8), 81.
Malde, H.E., 1968. The Catastrophic Late Pleistocene Bonneville Flood in the Snake River Plain, Idaho. U.S. Geological Survey, Reston, VA. 52 pp.
Morrison, R.B., 1991. Quaternary stratigraphic, hydrologic, and climatic history of the Great Basin, with emphasis on Lakes Lahontan, Bonneville, and Tecopa. In: Morrison, R.B. (Ed.), Quaternary Nonglacial Geology: Conterminous U.S. Geological Society of America, Golden, CO, pp. 283–320.
Mullineaux, D.R., 1986. Summary of pre-1980 tephra-fall deposits erupted from Mount St. Helens, Washington State, USA. Bulletin of Volcanology 48, 17–26.
Mullineaux, D.R., 1996. Pre-1980 Tephra-fall Deposits Erupted from Mount St. Helens, Washington. U.S. Geological Survey Professional Paper, vol. 1563. Reston, VA.
Negrini, R.M., 2002. Pluvial lake sizes in the northwestern Great Basin throughout the Quaternary Period. In: Hershler, R., Madsen, D.B., Currey, D.R. (Eds.), Great Basin Aquatic Systems History: Smithsonian Contributions to Earth Sciences. Smithsonian Institution Press, Washington, DC, pp. 11–52.
O'Connor, J.E., 1993. Hydrology, Hydraulics, and Geomorphology of the Bonneville Flood. Geological Society of America Special Paper vol. 274. Boulder, CO. 83 pp.
O'Connor, J.E., Webb, R.H., 1988. Hydraulic modeling for paleoflood analysis. In: Baker, V.R., Kochel, R., Patton, P.C. (Eds.), Flood Geomorphology. John Wiley and Sons, New York, NY, pp. 393–402.
O'Connor, J.E., Baker, V.R., 1992. Magnitudes and implications of peak discharges from glacial Lake Missoula. Geological Society of America Bulletin 104, 267–279.
O'Connor, J.E., Grant, G.E., Costa, J.E., 2002. The geology and geography of floods. In: House, P.K., Webb, R.H., Baker, V.R., Levish, D.R. (Eds.), Ancient Floods, Modern Hazards: Principles and Applications of Paleoflood Hydrology. American Geophysical Union, Washington, DC, pp. 359–385.
Oviatt, C.G., 1997. Lake Bonneville fluctuations and global climate change. Geology 25 (2), 155–158.
Personius, S.F., Crone, A.J., Machette, M.N., Kyung, J.B., Cisneros, H., Lidke, D.J., Mahan, S.A., 2004. Preliminary paleoseismology of the Steens Fault Zone, Bog Hot Valley, Nevada. Geological Society of America Abstracts with Programs 36 (5), 137.
Rathburn, S.L., 1993. Pleistocene cataclysmic flooding along the Big Lost River, east central Idaho. Geomorphology 8 (4), 305–319.
Reheis, M.C., 1999. Extent of Pleistocene lakes in the western Great Basin. U.S. Geological Survey Miscellaneous Field Studies Map MF-2323, scale 1:800,000.
Russell, I.C., 1884. A geological reconnaissance in southern Oregon. United States Geological Survey Annual Report 4, 431–464.
Russell, I.C., 1903. Preliminary Report on Artesian Basins in Southwestern Idaho and Southeastern Oregon. U. S. Geological Survey Water Supply Paper. Reston, VA. 53 pp.

Singleton, E.S., Oldow, J.S., 2004. Late Holocene deformation rates within the Alvord Basin, northwestern Great Basin, southwestern Oregon. Geological Society of America Abstracts with Programs 36 (4), 28.

Smith, W.D., Young, F.G., 1926. Physical and economic geography of Oregon: Chapter XI. The southeastern lake province. The Commonwealth Review. University of Oregon, Eugene, OR, pp. 218–219.

Walder, J.S., O'Connor, J.E., 1997. Methods for predicting peak discharge of floods caused by failure of natural and constructed earthen dams. Water Resources Research 33 (10), 2337–2348.

Walker, G.W., Repenning, C.A., 1966. Reconnaissance geologic map of the west half of the Jordan Valley Quadrangle, Malheur County, Oregon. U.S. Geological Survey Miscellaneous Field Investigations Map I-0457, scale 1:250,000.

Waitt, R.B., 1985. Case for periodic, colossal jökulhlaups from Pleistocene glacial Lake Missoula. Geological Society of America Bulletin 96, 1271–1286.